JOURNAL OF MATERIALS SCIENCE 20 (1985) 431–437

# Interfacial effects in carbon-epoxies

## Part 2 *Strength and modulus with short random fibres*

A. R. SANADI, M. R. PIGGOTT
*Department of Chemical Engineering and Applied Chemistry, University of Toronto, Toronto, Ontario M5S 1A4, Canada*

Random carbon fibre reinforced epoxy resin sheets have been prepared and tensile tested. The strengths and Young's moduli varied with fibre volume fraction and fibre length, but the values obtained were somewhat less than slip theory and shear lag theory would indicate. A new theory of slip, taking account of the angles between fibres and applied stress, but neglecting fibre–fibre interactions, predicts strengths and Young's moduli somewhat better.

### 1. Introduction

In randomly aligned short fibre composites, a good bond at the interface between fibres and matrix plays a major role in two processes: (1) transferring stress to fibres aligned close to the direction of any applied stress, and (2) ensuring that gaps do not open up between the matrix and fibres aligned at large angles to the stress directions.

Most of the studies on this type of composite have been carried out on very short (0.2 mm) fibre reinforced thermoplastic mouldings. Modulus is apparently not much affected by the bond between the fibres and matrix [1], but the strength is increased by good bonding [1]. However, a decline of modulus with time under load with a glass–polyester (thermoset) has been ascribed to loss in adhesion [2]. The reduction in strength when the composite is immersed in water is probably also due to loss of adhesion [3].

Strength and modulus are usually linear functions of fibre volume fraction [2–6] for reinforced thermoplastics and thermosets, though Weiss [7] observed a linear dependence for strength in injection moulded samples, which had some fibre alignment, but a nonlinear decrease in strength with fibre volume fraction for compression moulded samples, which had more randomly oriented fibres.

Stress–strain trajectories are normally curved [3, 4, 8], although Lavengood [6] reports linear stress–strain trajectories for (long) glass fibre mat reinforced epoxies.

The strengths of random fibre reinforced plastics can be less than the matrix strength [7, 9], and the effect of fibre aspect ratio on strength has been reported to be quite small [9] for aspect ratios ranging from 60 to 400.

It is implicit in theoretical treatments that we can treat the stress transfer from matrix to short fibres independently of the effect of the angle between the applied stress and the fibre direction [10, 11]. Thus, we write for composite Young's modulus, $E_c$:

$$E_c = \chi_1\chi_2 V_f E_f + V_m E_m \quad (1)$$

and for strength, $\sigma_{cu}$:

$$\sigma_{cu} = \chi_3\chi_4 V_f \sigma_{fu} + V_m \sigma_{mu} \quad (2)$$

where $V_f$ and $V_m$ are fibre and matrix volume fractions, $E_f$ and $E_m$ the corresponding Young's moduli, and $\sigma_{fu}$ and $\sigma_{mu}$ the strengths. The factors representing the effect of fibre orientation for modulus and strength are $\chi_1$ and $\chi_3$. For fibres randomly directed in a plane $\chi_1$ and $\chi_3$ are usually taken to be 3/8, and for the three dimensionally random case, 1/5. The factors used to account for the fibre length are $\chi_2$ and $\chi_4$. Shear lag analysis gives:

$$\chi_2 = 1 - \frac{\tanh(ns)}{ns} \quad (3)$$

0022–2461/85 $03.00 + .12 

and when account is taken of fibre slip [14], we get:

$$\chi_4 = 1 - \frac{s_c}{2s} \quad (4)$$

for fibre aspect ratios, $s$, greater than the critical aspect ratio, $s_c$, and:

$$\chi_4 = \frac{s}{2s_c} \quad (5)$$

for $s < s_c$. In Equation 3

$$n^2 = \frac{2E_m}{E_f(1+\nu_m)\ln\left(\frac{P_f}{V_f}\right)} \quad (6)$$

where $\nu_m$ is the Poisson's ratio of the matrix, and $P_f$ is the fibre packing factor. (For aligned fibres, hexagonally packed $P_f = 2\pi/3^{1/2}$).

Thus the equations predict a linear variation of modulus and strength with fibre volume fraction, as indeed most of the experiments indicate. However, curved stress–strain trajectories are not predicted, and the strength analysis is not compatible with that for the modulus.

In the experiments described here, the various factors contributing to strength and modulus are examined in a consistent and planned fashion as described previously for the aligned fibre case [15]. In addition, slip theory is extended to include the random fibre case, avoiding the assumption that the effects of short fibres, and fibre directions, are independent.

## 2. Experimental method

Union Carbide pitch precursor P55S fibres were used in this work. They were cut to 0.5, 1, 2, and 3 mm lengths for these experiments. As received, they were sized, but before use some were desized using propanol, others were desized and then etched with 70% nitric acid for 6 h, and still others were coated with silicone oil (Dow Corning 200). The critical lengths of these fibres were measured as described previously [15].

The resin matrix was Shell Epon 815, with 19% Ancamine 1482 added as hardener. The resin was cured at 100°C, and then post cured at 160°C for 4 h.

The mats were impregnated with the resin mixture dissolved in an equal amount of methylene chloride. Moulding was carried out after allowing the methylene chloride to evaporate. A pressure of 0.7 MPa was applied to the mould after the resin had been allowed to gel.

Testing was carried out as described previously [15]. In addition, the fibres were recovered from the composite and their lengths measured, as described previously.

## 3. Experimental results

To check for randomness, tests were carried out at 30°, 60° and 90° to the principal direction, as defined by the longer edges of the mould. The average strengths, measured on composite made with sized fibres, and $V_f = 0.15$, were the same within ± 6%.

During processing about 10% of the fibres were broken into fragments, Fig. 1, if we assume about two fragments for each fibre broken. (For example, for the 2 mm fibres about 7% had lengths less than 0.75 mm, 14.8% less than 1.25 mm, 16.5% less than 1.75 mm, and 20.7% less than 1.95 cm.)

The Young's moduli of the composites increased approximately linearly with fibre volume fraction, Fig. 2. The slope of the lines depended on fibre surface treatment, being greatest for the sized fibres and least for the silicone coated ones.

The modulus increased monotonically with fibre length, Fig. 3, up to 2 mm; increasing the fibre length to 3 mm had no significant effect. All the stress–strain curves were linear.

The tensile strengths increased monotonically with fibre volume fraction, Fig. 4. The highest strengths were obtained with the sized fibres, and the lowest with the silicone coated ones. At $V_f = 0.15$, the sized, desized and etched fibres all gave composites with about the same strengths. Strengths increased monotonically with increase in fibre length, Fig. 5, though the 2 mm and 3 mm fibre composites, had about the same strengths.

With the 2 mm long fibres the breaking strains

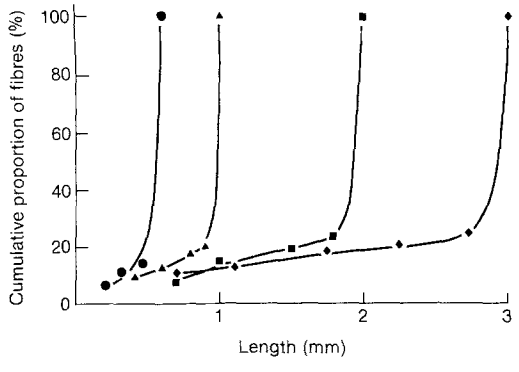


*Figure 1* Cumulative distribution of fibre lengths, $V_f = 0.30$.

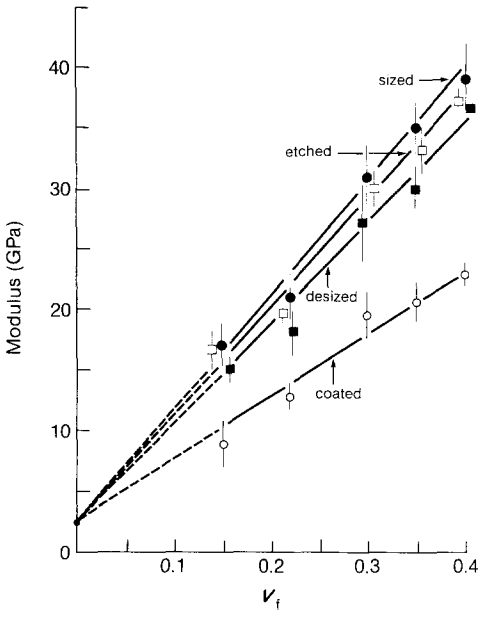


*Figure 2* Young's moduli of composites made with 2 mm long fibres.

of the composites decreased with increasing fibre volume fraction, from slightly above the fibre breaking strain (0.5%) to slightly below it, Fig. 6. The silicone coating reduced the composite breaking strain, for $V_f = 0.2$ to 0.4, and the

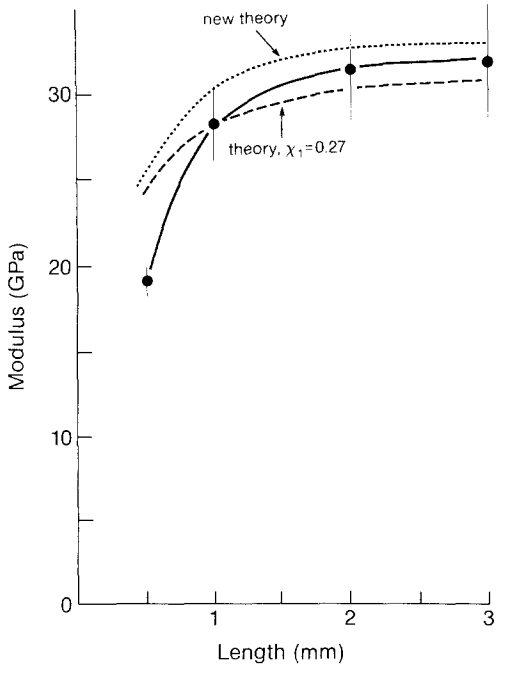


*Figure 3* Effect of fibre length on Young's moduli of composites with $V_f = 0.30$.

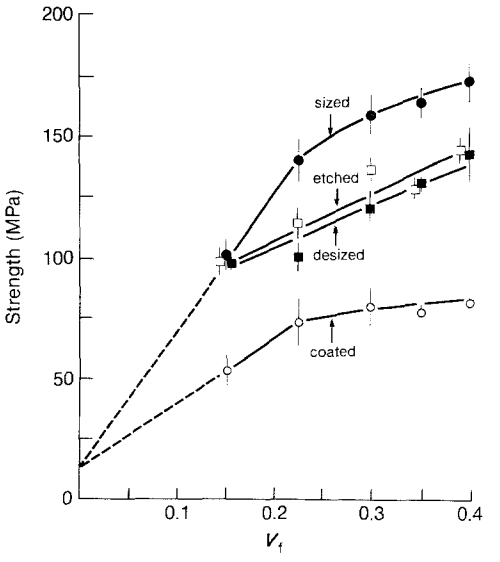


*Figure 4* Tensile strengths of composites made with 2 mm long fibres.

breaking strain increased approximately linearly with fibre length in the range of 0.5 to 3 mm, for $V_f = 0.3$.

## 4. Discussion

Fibre breakage, Fig. 1, is not occurring to any great extent in composite manufacture, so in our discussion we will use the nominal fibre lengths.

The moduli of the composites were linear

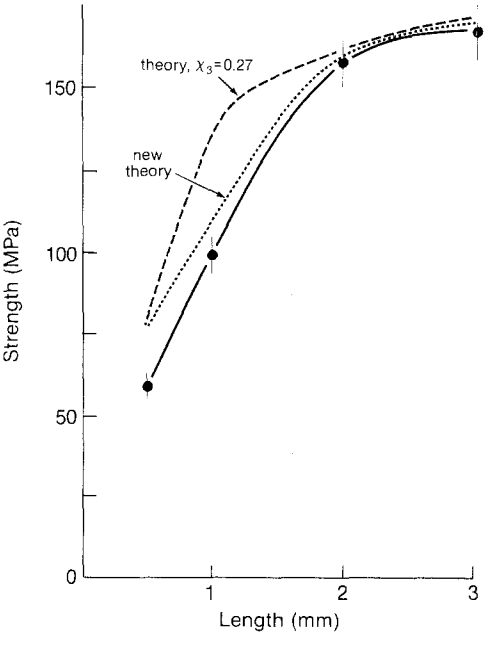


*Figure 5* Strength against fibre length, $V_f = 0.30$.

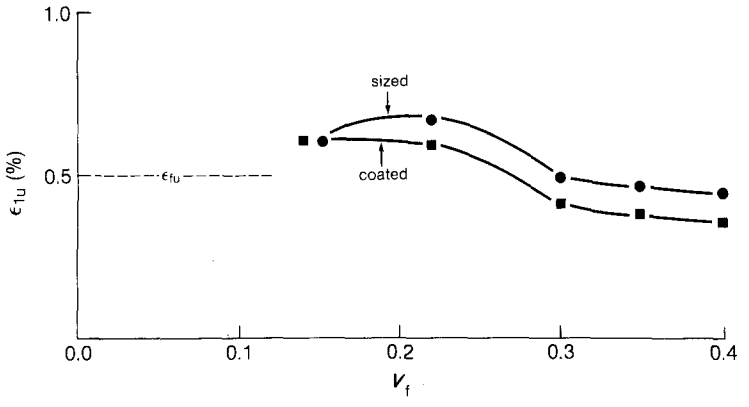


*Figure 6* Breaking strains of composites made with 2 mm long fibres.

functions of $V_f$, Fig. 2. Thus:

$$E_c = A_E V_f E_f + V_m E_m \quad (7)$$

where $A_E$ is a parameter which depends on fibre length and orientation. Values of $A_E$ estimated from Fig. 2 are given in Table I.

Comparing Equation 7 with Equation 1, we expect

$$A_E = \chi_1 \chi_2 \quad (8)$$

Values for $\chi_1$ and $\chi_2$ are also given in Table I, and it can be seen that Equation 8 is not obeyed. Agreement in the case of the sized fibres requires that $\chi_1$ be reduced to 0.21. This, however, still leaves a significant error in the desized fibre case, and a large error in the coated fibre case. Also, the variation of modulus with fibre length is not satisfactorily accounted for with $\chi_1 = 0.27$, Fig. 3. Thus shear lag theory, while in agreement with the linear stress–strain curves obtained, does not account very well for the modulus results.

This problem is not encountered when slip theory is used for the strength results at $V_f = 0.15$. The dashed lines in Fig. 4 were drawn according to the equation:

$$\sigma_{cu} = A_s V_f \sigma_{fu} + \frac{V_m E_m \sigma_{fu}}{E_f} \quad (9)$$

and are consistent with the results for the silicone coated fibres and the sized fibres at $V_f = 0.15$ and 0.20 only. For the etched and desized fibres Equation 9 breaks down even before $V_f$ reaches 0.20. If we estimate $A_s$ from the values at $V_f = 0.15$ and using the critical lengths given in the table [15] we get the results shown in Table I. Comparing Equations 9 and 2 we expect:

$$A_s = \chi_3 \chi_4 \quad (10)$$

In Table I, $\chi_3$ and $\chi_4$ values are given; the agreement in this case is quite good. However, at higher volume fractions the results fall below the values given by the slip theory, but if we use $\chi_3 = 0.27$ at $V_f = 0.3$, we obtain a theoretical curve which is reasonably close to the experimental one, Fig. 5. At this volume fraction we find that the composite breaking strains increase approximately linearly with fibre length, Fig. 7.

The breaking strains of the composites made with the coated fibres, Fig. 6, are less than those made with the sized fibres. This contrasts with the aligned fibre case [15], where the situation is reversed.

## 4.1. Slip theory for random composites

Since the assumption that orientation effects and short fibre effects act approximately independently gives moduli which are too high, even for sized fibres, it is worth investigating whether slip theory [16] can be adapted more rigorously to the

TABLE I Constants governing strength and modulus against fibre volume fraction plots (fibre length 2 mm)

| Fibre surface treatment | Critical length (mm) | Experiment $A_E$ | Modulus constants | | | Experiment $A_s$ | Strength constants | | |
|---|---|---|---|---|---|---|---|---|---|
| | | | $\chi_1$ | $\chi_2$ | $\chi_1\chi_2$ | | $\chi_3$ | $\chi_4$ | $\chi_3\chi_4$ |
| Sized | 0.73 | 25 | 0.38 | 0.93 | 0.35 | 30 | 0.38 | 0.80 | 0.30 |
| Desized | 0.91 | 23 | | | | 30 | | 0.75 | 0.29 |
| Etched | 0.89 | 24 | | | | 30 | | 0.76 | 0.29 |
| Coated | 1.80 | 14 | | | | 15 | | 0.51 | 0.19 |

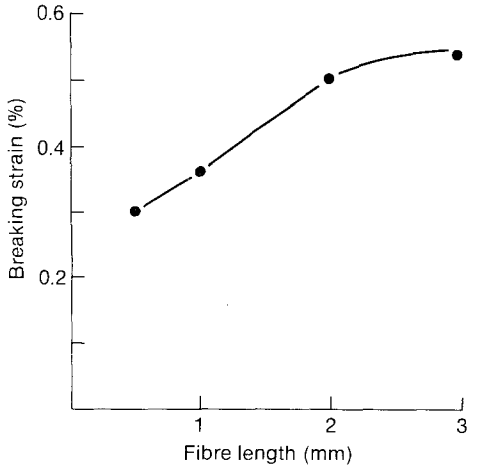


*Figure 7* Breaking strains of composites with $V_f = 0.30$.

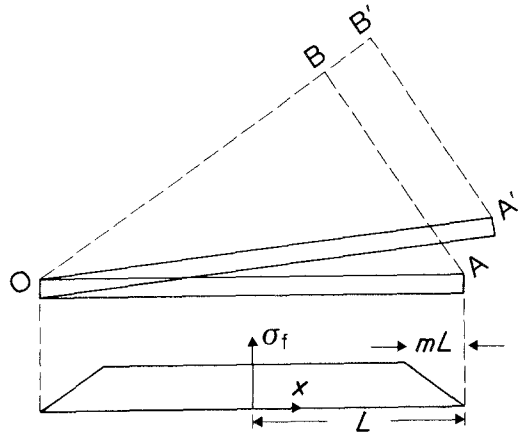


*Figure 8* Diagram showing fibre, $OA$ (initial position) stretched and rotated to $OA'$ by a stress applied in the direction $OB$. Also shown (lower left) is the variation of stress along the fibre.

random fibre case. To do this we will consider the usual single fibre model, Fig. 8.

We let the fibre, $OA$ be initially aligned at an angle $\theta$ to the applied stress $\sigma_1$. The stress will cause two effects: (1) an increase in the length of the space occupied by the fibre from $2L$ to $2L(1 + \epsilon_1)$, and (2) a rotation of the fibre due to Poisson's shrinkage of the composite. The strain in the composite in the direction of the applied stress is denoted by $\epsilon_1$.

To a first approximation, the distance $OB$ changes from $L\cos\theta$ to $OB' = L(1 + \epsilon_1)\cos\theta$. Similarly, the distance $AB = L\sin\theta$ changes to $A'B' = AB(1 - \nu_{12}\epsilon_1) = 2L(1 - \nu_{12}\epsilon_1)\sin\theta$ where $\nu_{12}$ is the Poisson's ratio of the sheet. The stretching and rotation results in a strain in the fibre, $\epsilon_f$, where

$$\epsilon_f = [(1 + \epsilon_1)^2\cos^2\theta + (1 - \nu_{12}\epsilon)^2\sin^2\theta]^{1/2} - 1 \quad (11)$$

which for small $\epsilon_f$ reduces to:

$$\epsilon_f = \epsilon_1[1 - (1 + \nu_{12})\sin^2\theta] \quad (12)$$

This results in fibres being under tension for $\theta < \phi$ and compression for $\theta > \phi$ where

$$\phi = \sin^{-1}\left[\frac{1}{(1 + \nu_{12})}\right]^{1/2} \quad (13)$$

The strain $\epsilon_f$ is only applied to the centre section of the fibres. Near the ends the stress, $\sigma_f$, falls approximately linearly to zero, as indicated in Fig. 8. In the end region, $x > L(1 - m_0)$, for fibres with $\phi = 0$ we have

$$\frac{d\sigma_f}{dx} = -\frac{4\tau_i}{d} \quad (14)$$

where $x$ is the distance from the fibre centre (Fig. 8), $d$ is the fibre diameter and $\tau_i$ is the interfacial shear stress resulting from slip. It is assumed that $\tau_i$ is constant. The fraction of fibres that have slipped, $m_0$ is given by [16]

$$m_0 = \frac{E_f\epsilon_1}{2s\tau_i} \quad (15)$$

where $s$ is the fibre aspect ratio, $2L/d$.

Fibres with $\theta < \phi$ will have

$$m_t = m_0[1 - (1 + \nu_{12})\sin^2\theta] \quad (16)$$

and those with $\theta > \phi$ will have

$$m_c = m_0[(1 + \nu_{12})\sin^2\theta - 1] \quad (17)$$

and the average stress in the fibre is

$$\bar{\sigma}_{f\theta} = \frac{E_f\epsilon_1 m_t\left(1 - \frac{m}{2}\right)}{m_0} \quad (18)$$

where $m = m_t$ for $\theta < \phi$ and $m = m_c$ for $\theta > \phi$.

Neglecting fibre–fibre interactions, the contribution $V_f\bar{\sigma}_{fl}$ of all fibres, at all angles, is obtained by integration:

$$V_f\bar{\sigma}_{fl} = \frac{2V_f}{\pi}\int_0^{\pi/2}\bar{\sigma}_{f\theta}\cos\theta\,d\theta \quad (19)$$

which may be integrated in two parts

$$V_f\bar{\sigma}_{fl} = \left(\frac{2V_f}{\pi}\right)\left(\frac{E_f\epsilon_1}{m_0}\right) \times\left[\int_0^{\phi} m_t\left(1 - \frac{m_t}{2}\right)\cos\theta\,d\theta + \int_{\phi}^{\pi/2} m_t\left(1 - \frac{m_c}{2}\right)\cos\theta\,d\theta\right] \quad (20)$$

to give:

$$V_f\bar{\sigma}_{f1} = \frac{V_f E_f \epsilon_1}{15\pi}\left\{10(2-\nu_{12}) - m_0 \times \left[\frac{16}{(1+\nu_{12})^{1/2}} - 8 + 4\nu_{12} - 3\nu_{12}^2\right]\right\} \quad (21)$$

We may likewise estimate the contribution of the fibres to the stresses in the plane of the sheet, at right angles to the fibre direction, $V_f\bar{\sigma}_{f2}$,

$$V_f\bar{\sigma}_{f2} = \frac{2V_f}{\pi}\int_0^{\pi/2}\bar{\sigma}_{f\theta}\sin\theta\,d\theta \quad (22)$$

$$= \frac{V_f E_f \epsilon_1}{15\pi}\left[10(1-2\nu_{12}) - m_0(3-4\nu_{12}+8\nu_{12}^2) - \frac{2m_0(3-10\nu_{12}+15\nu_{12}^2)}{(1+\nu_{12})^{1/2}}\right] \quad (23)$$

The matrix will also be stressed in this direction, since, for equilibrium

$$V_f\bar{\sigma}_{f2} + V_m\bar{\sigma}_{m2} = 0 \quad (24)$$

We identify the composite strain with the matrix strain

$$\epsilon_{2m} = -\nu_{12}\epsilon_1 \quad (25)$$

and the stress–strain relations give:

$$\sigma_{2m} = \frac{E_m}{(1+\nu_m)(1-2\nu_m)} \times [(1-\nu_m)\epsilon_{2m} + \nu_m(\epsilon_{1m} + \epsilon_{3m})] \quad (26)$$

so that, substituting $\epsilon_{2m}$ from Equation 25, putting $\epsilon_{1m} = \epsilon_1$, and $\epsilon_{3m} = -\nu_{13}\epsilon_1 \simeq \nu_m\epsilon_1$, we obtain:

$$\sigma_{2m} = \frac{E_m\epsilon_1(1-\nu_m)(\nu_m - \nu_{12})}{(1+\nu_m)(1-2\nu_m)} \quad (27)$$

Using Equations 23, 24 and 27 we find that $\nu_{12}$ is almost entirely independent of $m_0$, and given with great fidelity by

$$\nu_{12} = \frac{(1+\alpha\nu_m)}{(2+\alpha)} \quad (28)$$

where

$$\alpha = \frac{3\pi E_m V_m(1-\nu_m)}{2V_f E_f(1+\nu_m)(1-2\nu_m)} \quad (29)$$

For most fibre–matrix combinations, except at very low volume fractions, Equation 29 gives $\nu_{12} \simeq 0.5$.

The composite stress–strain relation, using Equations 15 and 21, and including a matrix contribution of $V_m E_m \epsilon_1$, is

$$\sigma_1 = \left\{\frac{V_f E_f}{15\pi}\left[10(2-\nu_{12}) - \frac{E_f\epsilon_1}{2s\tau_i} \times \left(\frac{16}{(1+\nu_{12})^{1/2}} - 8 + 4\nu_{12} - 3\nu_{12}^2\right)\right] + V_m E_m\right\}\epsilon_1$$

which, for $\nu_{12} = 0.5$, reduces to

$$\sigma_1 = \left[\frac{V_f E_f}{\pi}\left(1 - 0.21\frac{E_f\epsilon_1}{s\tau_i}\right) + V_m E_m\right]\epsilon_1 \quad (31)$$

This expression differs from the unidirectional slip equation [11] only by inclusion of the quotient $\pi$, and the multiplier 0.21 instead of 0.25.

Fig. 9 shows the theoretical stress–strain curves for the carbon-epoxy composites used in the experiments. The curves have been terminated at the breaking strains observed. The values of $m_0$ as well as fibre length are indicated on the curves. The breaking stresses are quite close to the values given by the theoretical curve, Fig. 5, when these breaking strains are used, and the secant moduli fit the Young's moduli fairly well, Fig. 3.

It seems clear that this theory comes closer to predicting the Young's moduli of these composites than does the treatment that considers angle and orientation effects separately. Thus to get the apparent agreement in Figs. 3 and 5, we had to reduce $\chi_1$ and $\chi_3$ to 0.27 (from 0.375). However, the new theory has two problems: (1) the stress–strain trajectories predicted are curved, while the experiments give linear trajectories, and (2) the theory lacks a criterion for determining the breaking strain for the composites made with very short fibres ($s < 1.4s_c$). It should be noted that, for fibres aligned normal to the direction of stress, the slipped length at the end of each fibre is about 0.12 mm long for both 0.5 and 1 mm fibres at the breaking point of the composite. This could constitute a critical crack size criterion.

These problems may be remedied, as indicated in the previous paper, by considering the fibre–fibre interactions. These interactions will probably also reduce the rather high value of $\nu_{12}$ that is predicted.

The new theory can be extended to the case $m_0 > 1$, i.e. the whole fibre is slipping. In this case

$$V_f\bar{\sigma}_{f1} \simeq 0.40V_f s\tau_i \quad (32)$$

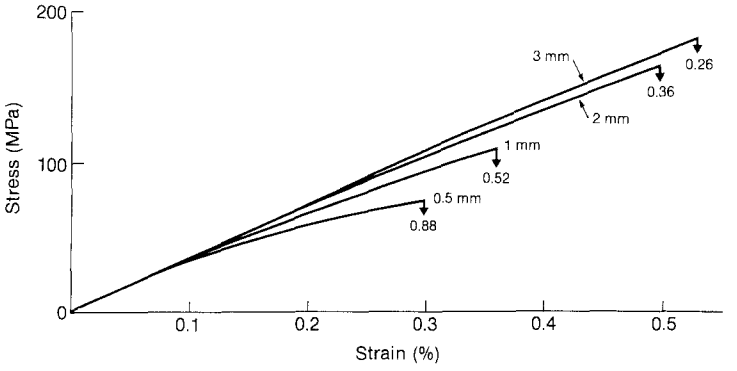


*Figure 9* Theoretical stress strain curves for short carbon fibre reinforced epoxies. $V_f = 0.30$. Fibre lengths (mm) and $m$ values indicated on the curves.

## 5. Conclusions

Simple slip and shear lag theories do not predict the strengths and Young's moduli of random, short fibre composites very well. A new theory, based entirely on slip, is better, and its deficiencies may be remedied by taking fibre–fibre interactions into account.


## Acknowledgements

The authors are grateful to Hartford Fibres, Kingston, Ontario, for cutting the fibres, and the Industrial Materials Research Institute (DSS contract No. 09SD-31155-1-5001) for financial support for this work.


## References


1. R. A. WEISS, *Polym. Comps.* **2** (1981) 89.
2. J. C. BAUWENS, J. P. DELIT and G. HOMES, *C.R. Acad. Sci. Paris* **264** (1967) 1909.
3. L. H. LEE, *Polym. Eng. Sci.* **9** (1969) 213.
4. N. SATO, S. SATO and T. KURANCHI, *Proc. ICCM4.* (1982) 1061.
5. N. TSUCHIYAMA, *Proc. ICCM4.* (1982) 497.
6. R. E. LAVENGOOD, *Polym. Eng. Sci.* **12** (1972) 43.
7. R. A. WEISS, *Polym. Comps.* **2** (1981) 95.
8. I. R. DOVER, I. O. SMITH and G. A. CHADWICK, *J. Mater. Sci.* **12** (1977) 1176.
9. M. MIWA, T. OHSAWA and K. TAHARA, *J. Appl. Polym. Sci.* **25** (1980) 795.
10. P. T. CURTIS, M. G. BADER and J. E. BAILEY, *J. Mater. Sci.* **13** (1978) 377.
11. M. R. PIGGOTT, "Load Bearing Fibre Composites" (Pergamon, Oxford, 1980) p. 102.
12. M. R. PIGGOTT, "Load Bearing Fibre Composites" (Pergamon, Oxford, 1980) p. 78.
13. H. L. COX, *Brit. J. Appl. Phys.* **3** (1952) 72.
14. A. KELLY and W. R. TYSON, *J. Mech. Phys. Solids* **13** (1965) 329.
15. A. R. SANADI and M. R. PIGGOTT, *J. Mater. Sci.* **20** (1985) 421.
16. M. R. PIGGOTT, "Load Bearing Fibre Composites" (Pergamon, Oxford, 1980) p. 62.



*Received 27 February 1984*
*and accepted 12 March 1984*